PAPER • **OPEN ACCESS**

SiC neutron detectors: enhancing the dynamic range through partial depletion operation

Plasma Physics and Controlled Fusion

OPEN ACCESS

RECEIVED
23 January 2026

REVISED
5 March 2026

ACCEPTED FOR PUBLICATION
31 March 2026

PUBLISHED
13 April 2026

PAPER

SiC neutron detectors: enhancing the dynamic range through partial depletion operation

Matteo Hakeem Kushoro[1,2,*], Gabriele Croci[1], Erik Gallo[3], Francesco La Via[4], Stefano Loreti[5], Enrico Perelli Cippo[2], Marica Rebai[2], Davide Rigamonti[2], Miriam Saleh[2], Marco Tardocchi[2], Letizia Giulietta Tedoldi[1], Salvatore Tudisco[6] and Massimo Nocente[1]

[1] Department of Physics 'Giuseppe Occhialini', University of Milano-Bicocca, Piazza dell'Ateneo Nuovo 1, 20126 Milano, Italy
[2] Institute for Plasma Science and Technology—CNR, Via Roberto Cozzi 53, 20125 Milano, Italy
[3] Eni S.p.A, Piazzale Mattei, 1–00144 Roma, Italy
[4] CNR-IMM, Strada VIII 5, 95121 Catania, Italy
[5] ENEA, Fusion and Technology for Nuclear Safety and Security Department, Via E. Fermi 45, 00044 Frascati, Italy
[6] Istituto Nazionale di Fisica Nucleare (INFN), Laboratori Nazionali del Sud (LNS), Via S. Sofia 62, Catania, 95123, Italy
[*] Author to whom any correspondence should be addressed.

E-mail: matteo.kushoro@unimib.it

Keywords: SiC, solid state detectors, fast neutrons, neutronics, Tokamak diagnostics

Abstract

Silicon Carbide (SiC) detectors are promising candidates for neutron diagnostics in fusion environments, where instruments must endure intense neutron and gamma fluxes, high temperatures, and restricted accessibility. Partial depletion operation enables online control of detector efficiency by varying the applied bias voltage, thereby tuning the response to adapt to the widely changing neutron fluxes expected in future Tokamak experiments. In this work, the functionality of two 4H-SiC detectors with different thicknesses (100 μm and 250 μm) is investigated under partial depletion conditions. Measurements are performed with 2.5 MeV and 14 MeV neutrons produced at the Frascati Neutron Generator and benchmarked against Geant4 simulations. Results show that detector efficiency can be predictably controlled within a factor of five without degrading energy resolution. Full depletion in the 100 μm device was reached at lower voltages than expected, possibly due to doping variations or irradiation effects. These findings confirm the potential of partial depletion as a tool for real-time tuning of SiC detector response, with significant implications for neutron diagnostics in future fusion reactors.

1. Introduction

Advancements in nuclear fusion are increasing the interest in diagnostic instruments capable of measuring the intense radiation produced in such experiments. Among these, neutron detectors are particularly interesting: by performing neutron counting and spectroscopy it is possible to assess various plasma parameters, like fusion power [1, 2], plasma shape [3, 4], fuel-ion ratio [5–7] and plasma ion temperature [1, 8]. Measuring neutrons will also be useful in assessing the production of tritium [9] in future machines featuring breeding elements, like ITER or Demo. Fast neutron detectors for fusion plasma, though, must be able to operate under the very high neutron and gamma fluxes expected in future Tokamaks—which, depending on the position and plasma regime, can be in the excess of 10^{13} cm^{-2} s^{-1} [10–12]. This requires them to be fast, resilient, gamma-transparent and with sizes that are compatible with the tight constraints of Tokamak environments. Because of that, solid state neutron detectors (SSDs) are an object of interest for research. Among SSDs, Silicon Carbide (SiC) detectors demonstrated good properties for neutron detection in harsh environments [13–16]. The SiC capability of operating both under full or partial depletion [17] promises good potential for a significant enhancement of its dynamic range by the means of changing its efficiency and thus adapting to the widely varying neutron fluxes on tokamaks [18].

The goal of this work is to expand the knowledge on partial depletion operation of SiC. This is achieved by measuring fast neutrons with two well characterized 4H-SiC detectors with different thicknesses while under different depletions. Results will be compared among themselves and with Geant4 simulation.

Section 2 will describe the experimental setup and the detector specifications, while section 3 will describe the simulation software and the neutron source. The response of the detector and the evolution of the detection characteristics as a function of depletion will be outlined in section 4. Conclusion and future perspectives will be discussed in section 5.

2. Detector and setup

SSDs are detectors constituted by a monocrystalline volume that serves both as a neutron conversion stage and as active detection volume. Their working principle involves a potential difference V_{bias} induced on the two ends of the crystal: since it has a high resistivity, no current is allowed to flow through it. The interaction of a fast neutron with a lattice nucleus either recoils (and ionizes) it, or triggers a nuclear reaction which generates charged products, like alpha particles or smaller nuclei: in either case, the secondary particles produced are charged and, thus, interact with the lattice structure generating a number of electron–hole pairs (e–h) proportional to their total energy (E_{d}). This abruptly reduce the resistivity of the lattice, allowing for a short ($\approx$ ns long) electric signal to be detected by the electronics. Since the number of e–h is proportional to E_{d}, this process allows for the detection of the neutron and the measurement of the energy it deposited in the active volume.

Silicon and Germanium detectors are popular options for SSDs due to the widely availability of electronic-grade material [19] and excellent performances [20], respectively. More recently, diamond established itself as the state of art for fast neutron detection with SSDs, due to its comparatively higher bandgap (5.5 eV) [21] and higher e-h production energy ($\simeq$ 13 eV) [22], which allowed it to reduce the noise induced by e–h generation due to temperature. Despite this, the very high purity requirements for the diamond pose manufacturing challenges [23], as well as posing some limitation on its stability [24] and its functionality at high temperatures [25].

Inversely polarized junctions (either p–n or Schottky) based on 4H-SiC based SSDs offer an alternative to diamond detectors. While retaining most of the advantages of diamond SSDs (featuring a relatively high bandgap of 3.2 eV and a e–h production energy of 8 eV [26]), SiCs demonstrated a better stability to irradiation [27] and a better performance at high temperatures when compared to diamonds [13, 28], all while having a simpler manufacturing process that allows their production in a larger array of geometries with lower costs [29]. Despite this, SiC also demonstrated a slightly worse energy resolution than diamond (between 2% and 3% with 14 MeV neutrons [30], against diamond's lower than 1% [31]) and a more complicated response function (due to competing nuclear reaction channels). These properties (better resilience but slightly worse performances) prospect SiC detectors to be good candidates specifically for harsh environments, like high temperature environments [13, 15].

An additional feature of the SiC detector derives from its junction structure. The detection of neutrons with SiC relies on the depleted region to be extended by the inverse bias voltage (V_{bias}) to the point of preventing current, effectively creating a solid ionization chamber. While the standard mode of operation expects a V_{bias} high enough for the depletion volume to extend to the entire active volume, previous studies demonstrated that detection is still possible with good detection properties even when the detector is not fully depleted [17, 18]. Such mode of operation, called 'Partial Depletion operation', might be a feature to extend the dynamic range of a particular SiC detector by the means of altering the absolute efficiency of the detector. This could be done by simply altering the V_{bias} to values lower than the one necessary for full depletion, thus causing the depletion region to extend to only a fraction of the entire width of the detector. The relation between the depletion region depth d and V_{bias} can be obtained from [32]:

$$d = \sqrt{\frac{2\epsilon_r\epsilon_0}{e} . \frac{V_{\text{bias}}}{n_D}}$$

where $\epsilon_r = 9.66$ is the SiC dielectric constant [33], ϵ_0 the vacuum permittivity, e the electron charge and n_D the density of donors (which, in first approximation, is equal to the n-side doping density). The depleted region, thus, extends only to a contiguous fraction of the volume of the detector, as depicted in figure 1. Since the efficiency of the detector depends linearly on the depleted volume, changing the V_{bias} directly changes the efficiency of the detector. Previous experiences suggests that the behavior of a partially depleted SiC mimics the behavior of a SiC having a thickness equal to the depleted region depth

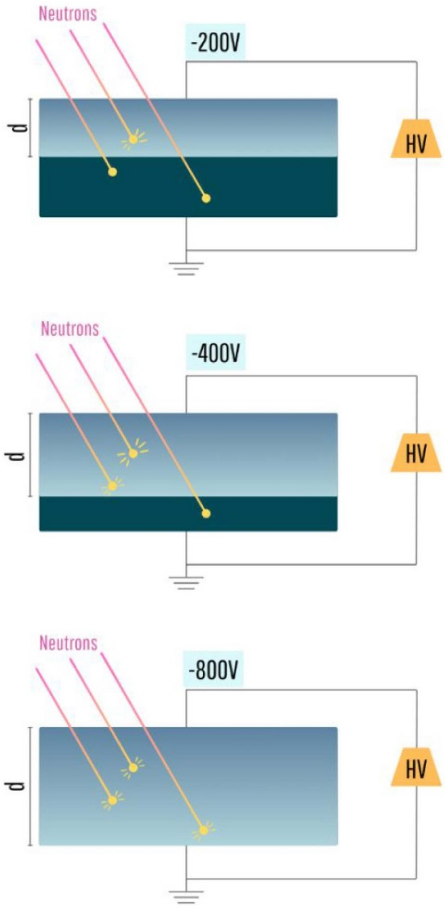

Figure 1. Schematic representation of the SiC active volume. The increase in V_{bias} progressively deplete a larger volume (light blue), increasing the chance of a neutron interacting with it and thus being detected. As a result, increasing V_{bias} also increases the efficiency of the detector.

d [17], with very few (if any) losses in detection quality [18]. This opens the possibility of altering the efficiency of the SiC online, allowing it to decrease its count rate when exposed to high fluxes (thus preventing pile-up and paralysation) or increase it when exposed to lower fluxes (thus preventing the lower detection rate also lowering the time resolution).

Previous works were performed on a 250 μm-thick SiCs that could not fully depleted (due to V_{bias} requirements incompatible with electronics). As such, the fully depleted and partially depleted behavior of the same SiC was never directly compared. To correct this, this study employs a 100 μm-thick SiC (SiC100) designed and manufactured at Istituto di Microelettronica e Microsistemi of the Italian National Research Council (IMM-CNR) within the SiCILIA collaboration [26, 34], which was already characterized in the past [30]. It also employs a 250 μm-thick SiC (SiC250) manufactured through a collaboration between INFN and IMM-CNR. Both detectors are shown in figure 2. SiC100 is made of a 2 $\times$ 2 grid of 5 mm $\times$ 5 mm independent active volumes, while SiC250 is made of two 2.5 mm $\times$ 5 mm independent active volumes. Only one active volume per detector was used for the experiment. SiC100 volume is made by a 0.3 μm-thin heavily doped (10^{19} cm^{-3}) p-region in contact with a 100 μm-thick n-region with a doping concentration of $5 \cdot 10^{13}$ cm^{-3} [34], while SiC250 junction is constituted by a Schottky contact and a n-doping concentration of $6 \cdot 10^{13}$ cm^{-3} [35].

The SiCs were coupled to a Cividec SiC preamplifier and its signal fed to a 500 MHz CAEN 5730 analog-to-digital converter. The electronics allowed the SiC100 to operate at the expected full depletion $V_{bias} = 460$ V.

The two SiCs were irradiated with neutrons while using various V_{bias}, in order to study the evolution of the efficiency and other detection characteristics as a function of V_{bias}. Two experimental activities were performed, during which the SiC100 was irradiated with 14 MeV neutrons, while SiC250 was irradiated with 2.5 MeV neutrons. The setup is described in the next section.

Figure 2. Picture of the two detectors used in this paper. On the left, the SiC100 features four 5 mm × 5 mm active volumes that can be seen in the center. A section of the aluminum casing can be seen on top. On the right, the two volumes of the SiC250 can be seen inside of their aluminum casing, connected to the Cividec preamplifier.

Figure 3. The SiC100 inside its aluminum casing installed on the FNG neutron source during the DT campaign. The 90° angle ensured that the neutrons reaching the detector had energy $E_n = 14.06$ MeV.

3. Data sources

The detectors were installed at the Frascati Neutron Generator (FNG), which produces fast neutrons by firing a deuterium beam against a target of either deuterium or tritium [36], thus producing deuterium–deuterium (DD) or deuterium–tritium (DT) fusion neutrons, respectively. The two detectors were installed on FNG in two different activities: the SiC250 was irradiated with DD neutrons while the SiC100 was irradiated by DT neutrons. In both instances the detector was placed with a 90° angle with respect of the deuterium beam, thus ensuring an irradiation by 2.45 MeV and 14.06 MeV neutrons, respectively [37]. In the case of the DT irradiation the detector was placed at a distance of approximately 20 cm at the same height of the target, while in the case of the DD irradiation it was placed below the target at an approximate distance of 15 cm. A picture showing the installation of the SiC100 on FNG is reported in figure 3. During the DT irradiation the SiC100 was placed both facing the neutron source and parallelly to the neutron source to study any effect due to the orientation, while the SiC250 was always kept facing the neutron source.

E_d spectra were collected in the form of histograms. Calibration in energy was performed for each spectrum on the known spectral features [30] and normalized on the number of neutrons fired by the

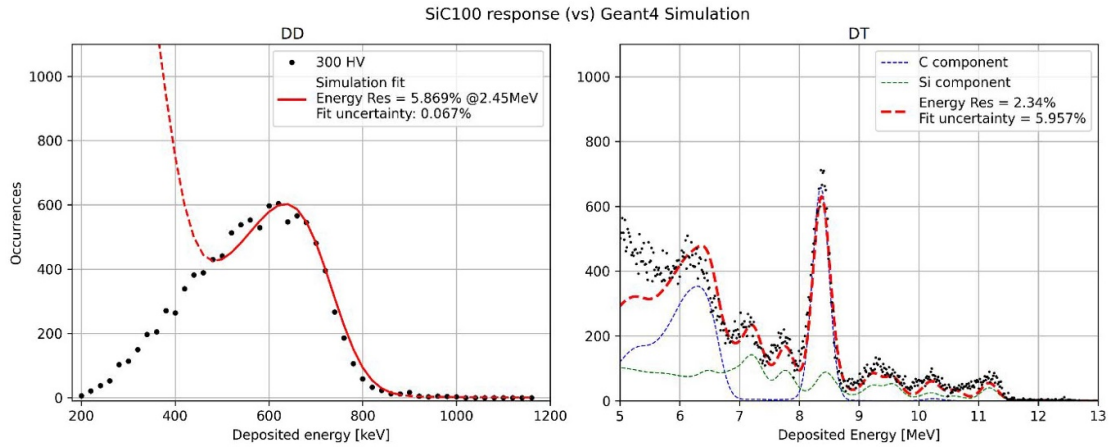

Figure 4. The SiC E_d spectra (in black) obtained under DD (left) and DT (right) neutron irradiation. Both spectra are obtained while using a $V_{bias} = 300$ V. Spectra are fitted with the synthetic data from Geant4 simulation (in red). Energy resolution is kept as a fitting parameter and is reported in the legends.

source (as measured by FNG control, which has a precision of ±3% for the DT neutrons and ±7% for the DD neutrons [38]). In order to extract information about the detection characteristics, E_d spectra were compared to numerical simulations obtained with the Geant4 software. The Geant4 version used was customized by Mikhail Osipenko in order to account for the correct behavior of the multi-body reaction of the neutron with carbon (detailed in [39] and [40]). It was also further customized to correctly account for the excited states of the Silicon (detailed in [41]). The Geant4 software was successfully compared against the experimental behavior of SiC detectors [41], thus validating its prediction. The synthetic data were then used to fit the E_d spectra, having only amplitude (a) and the amount of broadening σ as free parameters. More specifically:

- The amplitude a is a multiplicative factor applied to the histogram values, increasing all y-axis values by the same factor.
- The broadening is a process performed on synthetic data to account for the energy resolution of the detector. Each histogram bin is replaced by a Gaussian function having the same integral and a standard deviation equal to the energy resolution of the detector. Such standard deviation σ is used as a parameter of the fit.

The spectra are fitted with the synthetic data in the E_d regions that correspond to the most relevant spectral features: the elastic scattering on Carbon shoulder ($E_d = 0.7$ MeV) in the case of DD, and the $^{12}C(n,\alpha)^9Be$ nuclear reaction peak ($E_d = 8.3$ MeV) in the case of DT. The free fitting parameters a and σ are then used to monitor the reaction-related efficiency and the energy resolution of the detector with changing V_{bias}. Figure 4 shows two E_d spectra obtained during the DD and DT irradiation with the SiC250 and SiC100, respectively. A scan between 20 V and 475 V was performed on the SiC250, while a scan between 50 V and 800 V was performed during the SiC100 irradiation. Results are presented in the next section.

4. Results

The amplitude a and the broadening σ obtained by the fitting with simulation was calculated for all spectra. Their values as a function of V_{bias} are reported in figure 5 (SiC250 with DD neutrons) and figure 6 (SiC100 with DT neutrons), allowing to measure the change with V_{bias} of the reaction channel efficiency and the energy resolution of the detector.

Figure 5 shows that, for all the measured V_{bias}, the amplitude a of the fit follows the $a \sim \sqrt{V_{bias}}$ trend that is expected from the equation in section 2, while the broadening σ remains stable with changing V_{bias}. This confirms that the reaction efficiency can be controlled by the means of changing V_{bias} in a predictable and stable way over a factor 5 of efficiency, while keeping the energy resolution unaltered.

In the same way, figure 6 also shows that broadening remains stable over an even larger V_{bias} range (50–800 V). The reaction efficiency follows the $a \sim \sqrt{V_{bias}}$ trend that is expected from the equation in

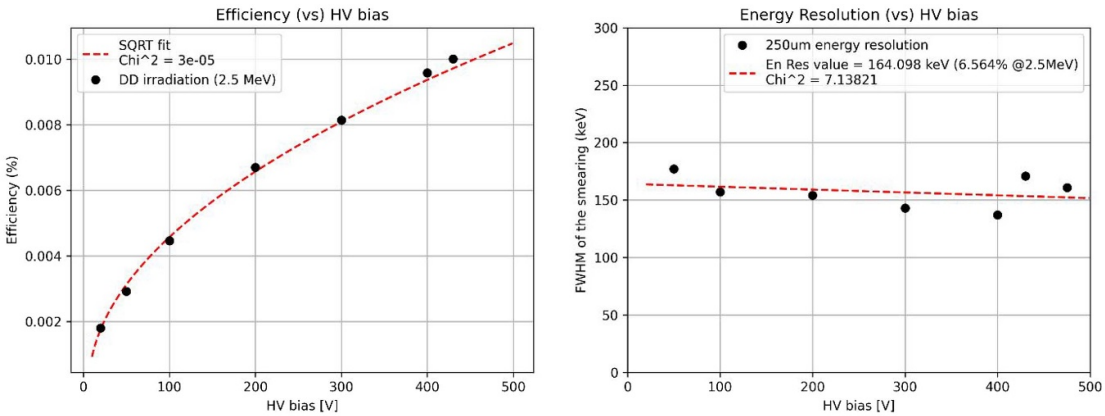

Figure 5. Value for the simulation fitting parameters as a function of for the SiC250 irradiated with DD neutrons. The efficiency, on the left, is measured from the elastic scattering on carbon spectral feature amplitude. On the right, the broadening of the same feature measures the energy resolution of the detector. The efficiency correlates very well with the expected $a \sim \sqrt{V_{\text{bias}}}$ derived from the equation in section 2, while the energy resolution remains stable with changing V_{bias}.

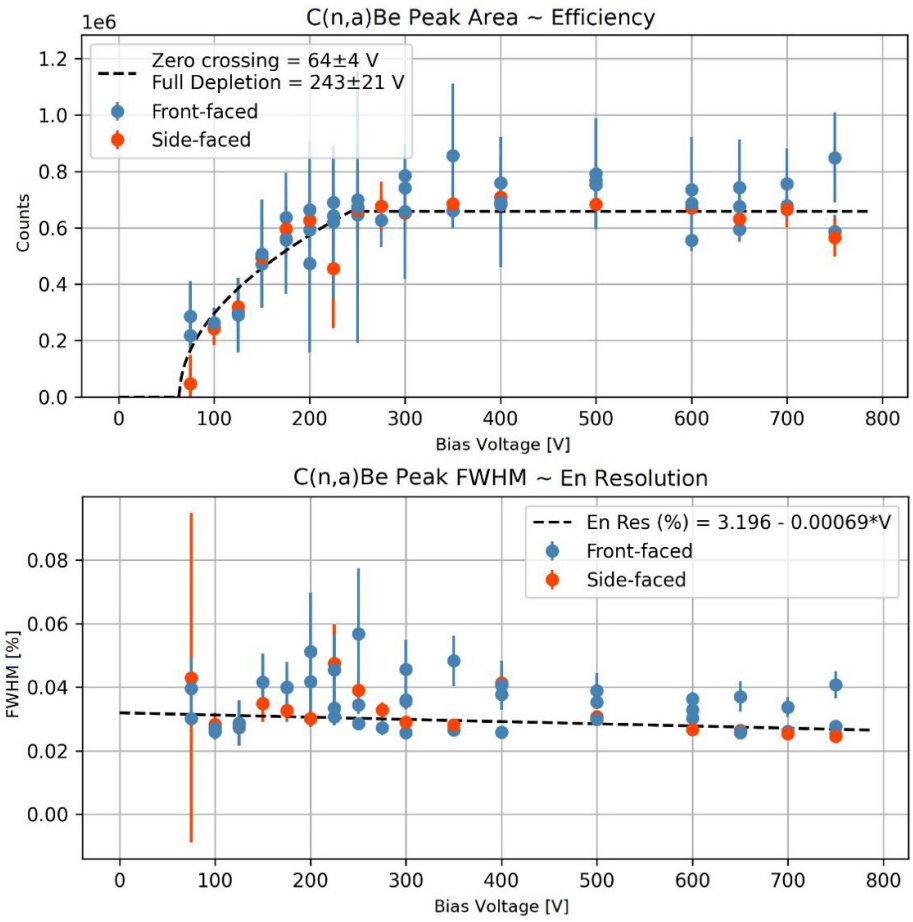

Figure 6. Fitting parameters value as a function of V_{bias} for the SiC100 irradiated with DT neutrons. The amplitude, on top, measures the efficiency for the $^{12}C(n,\alpha)^{9}Be$ reaction, while its FWHM, on bottom, measures the energy resolution of the detector. Efficiency follows the expected $a \sim \sqrt{V_{\text{bias}}}$ trend before reaching a plateau at $V_{\text{bias}} = 240$ V. Energy resolution is instead constant for all V_{bias} values. No difference can be seen between the data obtained with the detector surface perpendicular or parallel to the neutron paths.

section 2 up to a threshold V_{bias}, after which is replaced by a plateau ($a \sim \text{const}$), as expected when the detector reaches its full depletion. A root function combined with a horizontal function is used to fit such behavior, finding the threshold point at $V_{\text{bias}} \simeq 240$ V. This value is lower than the expected full depletion derived from the nominal detector characteristics ($V_{\text{bias}} = 460$ V). Two other fitting procedures were performed on the data (replacing the simulation fitting with a Gaussian fitting on the peak added

to a linear background and using the ^{28}Si(n,α)^{25}Mg spectral feature instead of the ^{12}C(n,α)^{9}Be) and the results obtained all agreed on a threshold point between 100 V and 300 V.

The proposed explanation is that, contrary to expectations of a full depletion achieved at $V_{\text{bias}} = 460$ V, this is reached at $V_{\text{bias}} \simeq 240$ V. By reversing equation 1, we obtain that a 100 μm depletion is achieved by a $V_{\text{bias}} \simeq 240$ V if the donor density is $n_D = 2.7 \cdot 10^{13}$ cm^{-3} (compared to the $n_D = 5 \cdot 10^{13}$ cm^{-3} density reported in [34]). The difference between the two measurements could either be due to a former incorrect evaluation of the doping level, or to neutron damage: the high neutron fluences experienced by the SiC100 during previous experimental campaigns, in fact, might have induced defects in the lattice acting as new acceptors, thus reducing the effecting donor density [42]. Both claims, though, could not be verified in this work, thus warranting further investigation.

5. Conclusions

The functionality of two well-characterized 100 μm-thick and 250 μm-thick SiC detectors was investigated with DD and DT fusion neutrons to compare their partial depletion functionality to their standard (i.e. fully depleted) functionality. Partial depletion operation was investigated as a mean to reduce the sensitive volume of the detector by altering the V_{bias}, which allows SiC to be tuned in efficiency through online means only (i.e., without replacing, moving, altering or otherwise 'shutting down' the detector). This could be very valuable in future Tokamak applications, being either research or power-producing machines, where the accessibility to near-to-plasma environments will be very limited and neutron fluxes are expected to vary by two orders of magnitude depending on plasma conditions (e.g. a 50%–50% DT plasma will produce 80 times more neutrons than a pure deuterium plasma, other factors being equal [43]).

The efficiency of the detectors was measured by fitting the E_{d} spectra at various V_{bias} with the result of a Geant4 numerical simulation already validated in the past [41]. The fit was performed on the most relevant spectral features (the shoulder of the elastic scattering on carbon for the DD irradiation and the ^{12}C(n,a)^{9}Be nuclear reaction for the DT irradiation). Two factors a and σ, measuring the amplitude and the broadening applied to the simulation, were kept as free parameters for the fitting and were used as a tool to measure the reaction channel efficiency and the energy resolution of the detector, respectively.

Results shows that the SiC's energy resolution is not altered with changing V_{bias} for the two detectors, confirming the invariability of SiC detection characteristics in partial depletion operation. The reaction channel efficiency, instead, scales linearly with $\sqrt{V_{\text{bias}}}$, as expected from theory, allowing to alter the efficiency by a factor of five. In the case of the SiC100, such scaling is interrupted at $V_{\text{bias}} = 240$ V, after which the efficiency reached a plateau. This behavior suggests that the full depletion of the detector is reached at V_{bias} lower that the expected necessary for full depletion ($V_{\text{bias}} = 460$ V). One possible explanation is that the neutron damage sustained by the detector over several experimental campaigns (before this one) induced lattice defects that act as acceptor levels, reducing the effective doping of the detector [42].

Results demonstrate that the partial depletion operation of SiC can indeed alter the efficiency of the detector in a predictable way while retaining all the performances of a fully depleted detector. On the other hand, further investigation should be performed to clarify the causes of the unexpected V_{bias} value required to fully deplete the detector—for example, by performing electronic measurements on the same detector and compare the measured n_D. Further test should also be conducted to assess possible changes in the p–n junction behavior after prolonged neutron irradiation.

Acknowledgments

This work was carried out within the framework of the Multilayered Urban Sustainability Action (MUSA), financed by the European Union—NextGenerationEU, PNRR Mission 4 Component 2, Investment Line 1.5: Creazione e rafforzamento degli 'ecosistemi dell'innovazione', costruzione di 'leader territoriali di R&S'. We would like to express our gratitude to the MUSA project and its contributors for their support and commitment to advancing research and innovation.

A special thanks is addressed to Mikhail Osipenko, whose contribution was essential for the development of the customized Geant4 software used for the synthetic results used in this paper.

Special thanks go also to the instrument scientists of the FNG facility, whose helpfulness was instrumental in acquiring the data and the experience needed to make this work possible. Special thanks go to Maurizio Angelone, Guglielmo Pagano, Antonino Pietropaolo and Mario Pilon.

Data availability statement

All data that support the findings of this study are included within the article (and any supplementary files).

Author contributions

Matteo Hakeem Kushoro 0000-0002-2859-8345
Conceptualization (lead), Data curation (lead), Formal analysis (lead), Investigation (lead), Methodology (lead), Software (lead), Visualization (lead), Writing – original draft (lead)

Gabriele Croci 0009-0004-3302-4209
Supervision (lead)

Erik Gallo 0009-0007-8554-9869
Funding acquisition (equal)

Francesco La Via 0000-0002-6842-581X
Resources (equal)

Stefano Loreti 0000-0003-1888-2921
Investigation (supporting), Resources (equal)

Enrico Perelli Cippo 0000-0002-8151-3427
Investigation (supporting)

Marica Rebai 0000-0002-0247-9073
Conceptualization (supporting), Supervision (supporting)

Davide Rigamonti 0000-0003-0183-0965
Investigation (supporting)

Miriam Saleh 0000-0001-5825-5012
Visualization (supporting)

Marco Tardocchi 0000-0001-8443-1809
Project administration (supporting)

Letizia Giulietta Tedoldi 0009-0001-7664-2291
Investigation (supporting)

Salvatore Tudisco 0000-0002-9390-9912
Resources (equal)

Massimo Nocente 0000-0003-0170-5275
Funding acquisition (equal), Project administration (equal)

References

[1] Ericsson G 2019 Advanced neutron spectroscopy in fusion research *J. Fusion Energy* **38** 330–55
[2] Esposito B *et al* 2022 Progress of design and development for the ITER radial neutron camera *J. Fusion Energy* **41** 22
[3] Bielecki J and Kurowski A 2019 Neutron diagnostics for Tokamak plasma: from a plasma diagnostician perspective *J. Fusion Energy* **38** 386–93
[4] Popovichev S *et al* 2008 Neutron emission profile and neutron spectrum measurements at jet: status and plans *AIP Conf. Proc.* **988** 275–82
[5] Vingren B *et al* 2025 Deuterium and tritium density determination at JET using neutron diagnostics *Nucl. Fusion* **65** 096025
[6] Scholz M *et al* 2019 Conceptual design of the high resolution neutron spectrometer for ITER *Nucl. Fusion* **59** 065001
[7] Tardocchi M *et al* 2022 A high-resolution neutron spectroscopic camera for the SPARC Tokamak based on the jet European torus deuterium-tritium experience *Rev. Sci. Instrum.* **1** 113512
[8] Hellesen C, Eriksson J, Binda F, Conroy S, Ericsson G, Hjalmarsson A, Skiba M and Weiszflog M 2015 Fuel ion ratio determination in NBI heated deuterium tritium fusion plasmas at JET using neutron emission spectrometry *Nucl. Fusion* **55** 023005
[9] Fonnesu N *et al* 2024 Measurement of tritium production in the helium cooled pebble bed test blanket module mock-up at JET during DTE2 *Eur. Phys. J. Plus* **139** 893
[10] Noce S *et al* 2024 Nuclear analyses for the integration of ITER equatorial Port 2 *Fusion Eng. Des.* **202** 114286
[11] Luís R *et al* 2023 Neutronics simulations for DEMO diagnostics *Sensors* **23** 5104
[12] Gilbert M R, Dudarev S L, Zheng S, Packer L W and Sublet J-C 2012 An integrated model for materials in a fusion power plant: transmutation, gas production, and helium embrittlement under neutron irradiation *Nucl. Fusion* **52** 083019

[13] Kushoro M H et al 2025 Fast neutron spectroscopy with 4H-SiC solid-state detectors up to 500 °C for nuclear fusion applications Meas. Sci. Technol. 36 125901
[14] Ruddy F H, Ottaviani L, Lyoussi A, Destouches C, Palais O and Reynard-Carette C 2021 Performance and applications of silicon carbide neutron detectors in harsh nuclear environments EPJ Web Conf. 253 11003
[15] Kushoro M H et al 2024 Operation of a 250μm-thick SiC detector with DT neutrons at high temperatures Fusion Eng. Des. 204 114486
[16] Meli A, Muoio A, Trotta A, Meda L, Parisi M and La Via F 2021 Epitaxial growth and characterization of 4H-SiC for neutron detection applications Materials 14 976
[17] Kushoro M H, Rebai M, La Via F, Meli A, Meda L, Parisi M, Cippo E P, Putignano O, Trotta A and Tardocchi M 2023 "Performance of a thick 250 μm silicon carbide detector: stability and energy resolution J. Instrum. 18 C03007
[18] Kushoro M H, Angelone M, Bozzi D, Gorini G, La Via F, Perelli Cippo E, Pillon M, Tardocchi M and Rebai M 2024 Partially depleted operation of 250 μm-thick silicon carbide neutron detectors Nucl. Instrum. Methods Phys. Res. A 1058 168918
[19] Von Ammon W and Herzer H 1984 The production and availability of high resistivity silicon for detector applications Nucl. Instrum. Methods Phys. Res. 226 94–102
[20] Flakus F N 1982 Detecting and measuring ionizing radiation—a short history IAEA Bull. 23 31-6
[21] Clark C D, Dean P J and Harris P V 1964 Intrinsic edge absorption in diamond Proc. R. Soc. London Ser. A 277 312–29
[22] Kraus B, Steinegger P, Aksenov N V, Dressler R, Eichler R, Griesmayer E, Herrmann D, Türler A and Weiss C 2021 Charge carrier properties of single-crystal CVD diamond up to 473 K Nucl. Instrum. Methods Phys. Res. A 989 164947
[23] Rodgers L V H, Hughes L B, Xie M, Maurer P C, Kolkowitz S, Bleszynski Jayich A C and de Leon N P 2021 Materials challenges for quantum technologies based on color centers in diamond MRS Bull. 46 623–33
[24] Rebai M, Fazzi A, Cazzaniga C, Croci G, Tardocchi M, Perelli Cippo E, Frost C D, Zaccagnino D, Varoli V and Gorini G 2016 Time-stability of a single-crystal diamond detector for fast neutron beam diagnostic under alpha and neutron irradiation Diam. Relat. Mater. 61 1–6
[25] Angelone M and Verona C 2021 Properties of diamond-based neutron detectors operated in harsh environments J. Nucl. Eng. 2 422–70
[26] Tudisco S et al 2018 SiCILIA—Silicon carbide detectors for intense luminosity investigations and applications Sensors 18 2289
[27] Kushoro M H et al 2021 Detector response to D-D neutrons and stability measurements with 4H silicon carbide detectors Materials 14 568
[28] Szalkai D, Ferone R, Issa F, Klix A, Lazar M, Lyoussi A, Ottaviani L, Tutto P and Vervisch V 2016 Fast neutron detection with 4h-sic based diode detector up to 500 °C ambient temperature IEEE Trans. Nucl. Sci. 63 1491–8
[29] De Napoli M 2022 SiC detectors: a review on the use of silicon carbide as radiation detection material Front. Phys. 10 898833
[30] Kushoro M H et al 2020 Silicon Carbide characterization at the n_TOF spallation source with quasi-monoenergetic fast neutrons Nucl. Instrum. Methods Phys. Res. A 983 164578
[31] Rigamonti D et al 2018 Neutron spectroscopy measurements of 14 MeV neutrons at unprecedented energy resolution and implications for deuterium–tritium fusion plasma diagnostics Meas. Sci. Technol. 29 045502
[32] Knoll G F 2010 Radiation Detection and Measurement 4th edn (Wiley) p 217
[33] Patrick L and Choyke W J 1970 Static dielectric constant of SiC Phys. Rev. B 2 2255–6
[34] Tudisco S et al 2019 Silicon carbide for future intense luminosity nuclear physics investigations Nuovo Cimento Soc. Ital. Fis., C 42 74
[35] Trovato G et al 2024 250 μm thick detectors for neutron detection: design, electrical characteristics, and detector performances Key Eng. Mater. 984 35–40
[36] Martone M, Angelone M and Pillon M 1994 The 14 MeV Frascati neutron generator J. Nucl. Mater. 212–215 1661–4
[37] Angelone M, Pillon M, Batistoni P, Martini M, Martone M and Rado V 1996 Absolute experimental and numerical calibration of the 14 MeV neutron source at the Frascati neutron generator Rev. Sci. Instrum. 67 2189–96
[38] Pietropaolo A et al 2018 The Frascati neutron generator: a multipurpose facility for physics and engineering J. Phys.: Conf. Ser. 1021 012004
[39] Osipenko M, Ripani M, Ricco G, Caiffi B, Pompili F, Pillon M, Verona-Rinati G and Cardarelli R 2016 Response of a diamond detector sandwich to 14 MeV neutrons Nucl. Instrum. Methods Phys. Res. A 817 19–25
[40] Osipenko M et al 2018 Upgrade of the compact neutron spectrometer for high flux environments Nucl. Instrum. Methods Phys. Res. A 883 14–19
[41] Kushoro M et al 2025 SiC detector response to Tokamak neutron spectra mock-up validated on experimental results Fusion Eng. Des. 214 114875
[42] Mancuso A S et al 2025 Defects induced by high-temperature neutron irradiation in 250 μm-Thick 4H-SiC p-n junction detector Materials 18 2413
[43] Forrest C J et al 2017 First measurements of deuterium-tritium and deuterium-deuterium fusion reaction yields in ignition-scalable direct-drive implosions Phys. Rev. Lett. 118 095002